2020 IEEE/RSJ International Conference on Intelligent Robots and Systems (IROS)
October 25-29, 2020, Las Vegas, NV, USA (Virtual)

# Design of a Linear Gravity Compensator for a Prismatic Joint

Do-Won Kim, Won-Bum Lee, and Jae-Bok Song, *Senior, IEEE*

**Abstract - Most existing mechanical gravity compensators have been developed for revolute joints that are found in majority of articulated robot arms. However, robots such as patient transport robots use prismatic joints, which need to handle a heavy payload. In this study, a high-capacity linear gravity compensator (LGC), which comprises pure mechanical components, such as coil springs, a rack-pinion gear, a cam, and a wire, is proposed to compensate for the payload applied to a prismatic joint. The LGC is designed to generate a constant compensation force regardless of the payload position. The device can be manufactured at a low cost and has a significantly long lifespan because it uses coil springs to serve as an elastic body. Experiments demonstrate that the robot with the LGC can handle a load of 100 kg more than the robot using the same motors without it.**

## I. Introduction

Most articulated robot arms comprise revolute joints, and motor torque is mostly used to support their own body weight. As the weight and payload of a robot increase, the torque required for the robot operation also increases, thus requiring a high-capacity motor and speed reducer. Several gravity-compensation techniques have been proposed to compensate for the gravitational torque applied to robot joints. Among such devices, counterweights, coil springs, and gas springs are typically used for gravity compensation [1–4], and research on the design of more compact and efficient gravity-compensation devices is currently underway [5-8].

However, these studies on gravity compensation have focused only on revolute joints, which makes their application to robots with prismatic joints perpendicular to the ground challenging. Because several service robots with prismatic joints, such as PR-2 and SASUKE [9, 10], have been developed recently, the demand for such linear gravity compensators (LGCs) is increasing.

LGCs are expected to generate a constant compensation force regardless of the load position because prismatic joints perpendicular to the ground are subject to constant gravity unlike revolute joints. A constant load spring produces a constant restoring force regardless of the spring tension length [11]. This spring has the advantage of generating a considerably large restoring force in comparison with its volume; however, it is not suitable for robots that need to be driven for a long time because its life is shorter than 10,000 cycles. Another device that provides a constant force in the linear direction is a spring balancer with a power spring [12]. However, the spring balancer has a large volume and weight in comparison with its payload, and its lifetime is not long owing to the nature of the power spring, rendering the spring balancer unsuitable for robotic applications. A device suitable for prismatic joints was studied in [13] using the difference in spring forces between two springs. However, this device is bulky in comparison with the compensation force generated because the elastic forces of the two springs cannot be used to their full potential to support the weight and are lost in the process of canceling each other's spring forces.

To overcome this problem, a high-capacity LGC is developed in this study; it consists of coil springs, a rack-and-pinion, a cam, and a wire. The proposed LGC is designed to compensate for the gravity in the vertical direction by generating a constant compensation force regardless of the payload position. The use of coil springs instead of constant load springs or power springs results in the significantly long lifetime of the LGC (more than 1 million cycles) and enables the LGC to generate a high compensation force of approximately 1,000 N. Owing to these characteristics, the LGC can be mounted inside a robot with a prismatic joint perpendicular to the ground, enabling the realization of a large payload with a low-capacity motor.

The rest of this paper is organized as follows. Section II presents the principle of operation and the design of the proposed LGC. In section III, the gravity compensation performance of the robot is investigated through experiments. Finally, conclusions are drawn in section IV.

## II. Linear Gravity Compensator

### A. Principle of LGC

Prismatic joints perpendicular to the ground are subjected to a constant magnitude of gravity, and the spring force of a coil spring increases in proportion to the compression, as illustrated in Fig. 1 (a). Therefore, for the gravity compensation of prismatic joints, a device is needed to convert the spring force into a constant compensation force regardless of linear displacement, as depicted in Fig. 1 (b).

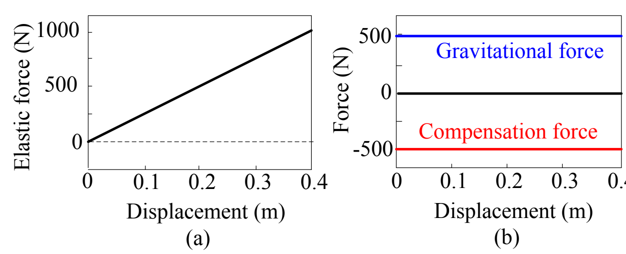


Figure 1. (a) Spring force of coil spring, and (b) constant gravitational force for prismatic joint.

* This research was supported by the MOTIE under the Care Robot Technology Development Program supervised by the KEIT (No. 20005002)

Do-Won Kim and Won-Bum Lee are with the School of Mechanical Eng., Korea University, Seoul, Korea (e-mail: ehdnjs119@korea.ac.kr).

Jae-Bok Song (corresponding author) is a Professor of the School of Mechanical Eng., Korea University, Seoul, Korea (Tel.: +82 2 3290 3363; fax: +82 2 3290 3757; e-mail: jbsong@korea.ac.kr).

The LGC proposed in this study is composed of a spring, cam-shaped wire guide, and rack-and-pinion, as depicted in Fig. 2(a). The wire guide and pinion are connected coaxially. The wire is fixed at one end of the wire guide, and then wound and released along the wire guide. As depicted in Fig. 2(b), the wire guide and pinion rotate by an angle $\theta$ when the load on the wire moves in the direction of gravity. The rack gear compresses the spring as it is moved by the rotation of the pinion, and produces a spring force.

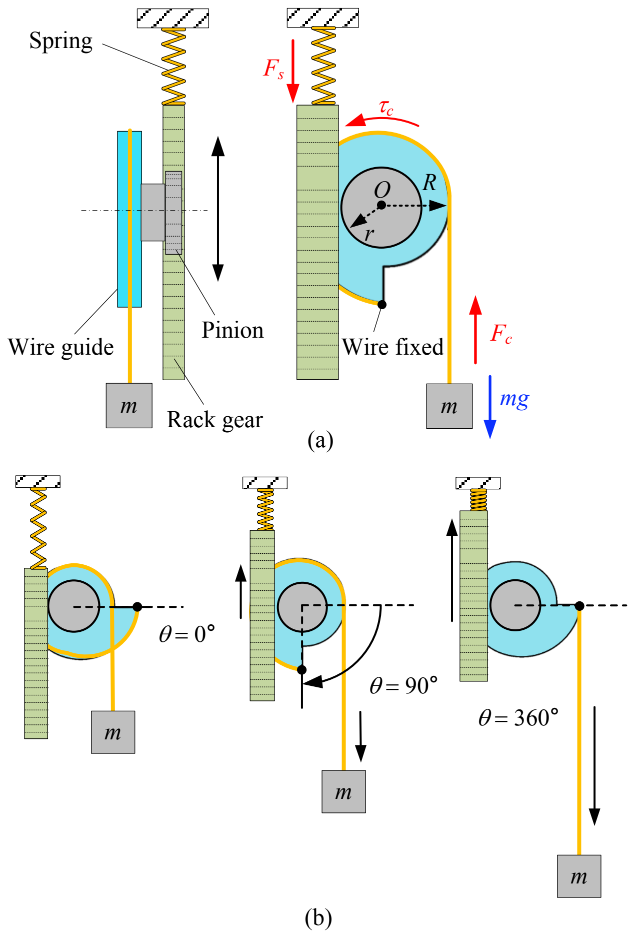


Figure 2. (a) Schematic of LGC, and (b) spring compression as a function of load position

The spring force $F_s$ of the coil spring is proportional to the compression length, and the spring is further compressed by the motion of the rack gear in addition to the initial compression as follows:

$$F_s = k(s + s_0) \tag{1}$$

where $k$ is the spring constant, $s_0$ is the initial compression length of the spring, and $s$ is the additional compression length caused by the movement of the rack gear. The travel distance of the rack gear is proportional to the rotation angle of the pinion with a radius of $r$, as follows:

$$s = r\theta \tag{2}$$

The compensation torque $\tau_c$ generated when a spring force $F_s$ is applied to the pinion through the rack gear can be expressed by

$$\tau_c = F_s r = kr(r\theta + s_0) \tag{3}$$

The wire is released by the rotation of the wire guide coupled with the pinion, and the compensation force $F_c$ applied to the wire is given by

$$F_c = \frac{\tau_c}{R} = \frac{kr(r\theta + s_0)}{R} \tag{4}$$

where $R$ is the radius of the wire guide. For complete gravity compensation, the compensation force $F_c$ should be equal to the gravity $mg$ due to the load as follows:

$$F_c = mg \tag{5}$$

Substitution of Eq. (5) into (4) yields

$$R = \frac{krs_0}{mg} + \frac{kr^2}{mg}\theta \tag{6}$$

Therefore, if $R$ is designed to be proportional to $\theta$, then the constant compensation force equal to the load can be obtained regardless of the payload position.

The operating distance $l$ of the LGC is the total length of the wire winding, which is equal to the cam circumference of the wire guide, and is calculated as

$$l = \int_0^{2\pi} R d\theta = \frac{2kr\pi}{mg}(r\pi + s_0) \tag{7}$$

Therefore, for the load $mg$ and the operating distance $l$ to be compensated, the LGC can be implemented by adjusting the design variables $k$, $r$, and $s_0$ of the gravity compensation mechanism and the cam shape $R(\theta)$ of the wire guide to satisfy Eq. (6) and (7).

### B. *Design Parameters of LGC*

The wire guide is a cam structure in which the radius $R$ linearly increases in proportion with the rotation angle $\theta$. Unlike in the circular structure, the tangential line and the cam radius are not perpendicular to each other, and thus the radius of the wire guide does not perfectly match the moment arm. When the wire is pulled and the cam is rotated by $\theta$, as depicted in Fig. 3, the actual contact P of the wire and cam does not lie on the horizontal line, and the line OP and the horizontal line OA are at an angle of $\alpha$. The length of OP can be obtained from Eq. (6) as follows:

$$\overline{OP} = \frac{krs_0}{mg} + \frac{kr^2}{mg}(\theta + \alpha) \tag{8}$$

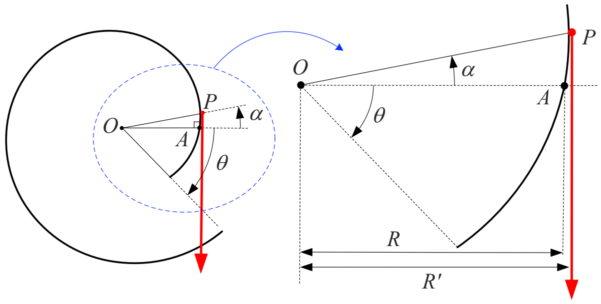


Figure 3. Geometry of cam rotated by $\theta$

Considering $R' = OP\cos\alpha$, the following relation is obtained.

$$R' = \frac{krs_0}{mg}\cos\alpha + \frac{kr^2}{mg}(\theta+\alpha)\cos\alpha \tag{9}$$

Since the wire extends in the tangential direction perpendicular to the cam, the value of $R'$ is at its maximum at the point at which $dR'/d\alpha = 0$ as follows:

$$-\frac{krs_0}{mg}\sin\alpha + \frac{kr^2}{mg}\cos\alpha - \frac{kr^2}{mg}(\theta+\alpha)\sin\alpha = 0 \tag{10}$$

This equation can be simplified to

$$s_0\sin\alpha + r(\theta+\alpha)\sin\alpha - r\cos\alpha = 0 \tag{11}$$

Assuming that $\alpha$ is sufficiently small, substituting $\sin\alpha \approx \alpha$, $\cos\alpha \approx 1$ into Eq. (11) yields

$$r\alpha^2 + (s_0 + r\theta)\alpha - r = 0 \tag{12}$$

Thus, $\alpha$ is given by

$$\alpha = \sqrt{\left(\frac{s_0}{2r}+\frac{\theta}{2}\right)^2 + 1} - \left(\frac{s_0}{2r}+\frac{\theta}{2}\right) \tag{13}$$

Therefore, $\alpha$ approaches zero as $s_0/2r$ increases. To approximately quantify the aforementioned analysis, the error $e$ defined below is computed in the case where $s_0$ is two, four, and six times the value of $r$ for the range of $0 \le \theta \le 2\pi$.

$$e = \frac{R'-R}{R} \times 100(\%) \tag{14}$$

As illustrated in Fig. 4, the larger $s_0$ is in comparison with $r$, the smaller the error is between the moment arm and the cam radius of the compensation torque. When $s_0 = 4r$, the error is found to be less than approximately 3%, implying that if the initial compression length of the spring is more than four times the pinion radius, the LGC can generate a uniform compensation force with more than 97% accuracy.

$$s_0 > 4r \tag{15}$$

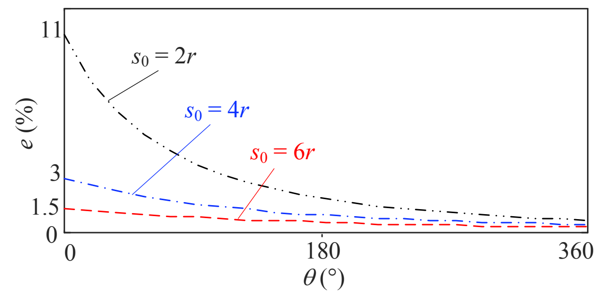


Figure 4. Moment arm error according to ratio of $s_0$ to $r$

### C. Fabrication of LGC

The actual LGC is designed based on the analysis detailed in the previous section, as illustrated in Fig. 5(a). The LGC is compactly designed to be mounted inside the robot while simultaneously targeting a compensation force of 1,000 N ($mg$) and an operating distance of 400 mm ($l$). The LGC is equipped with a 190 × 20 mm wire guide on a 450 × 200 × 80 mm main body and has a mass of 10 kg. The rack-and-pinion is placed between the two springs to prevent the moment due to the restoring force of the springs from being pulled to one side. The wire guides are made with $\phi$ 190 mm disks on both sides of the cam to prevent the wires from escaping. The design variables are chosen as $k = 15.6$ N / mm, $s_0 = 100$ mm, and $r = 22.5$ mm. The radius $R$ of the cam is depicted in Fig. 5 (b). The compensation force expected by the design variables is approximately 1003 N. Figure 6 illustrates the rotation of the wire guide and the compression of the spring as the wire is pulled.

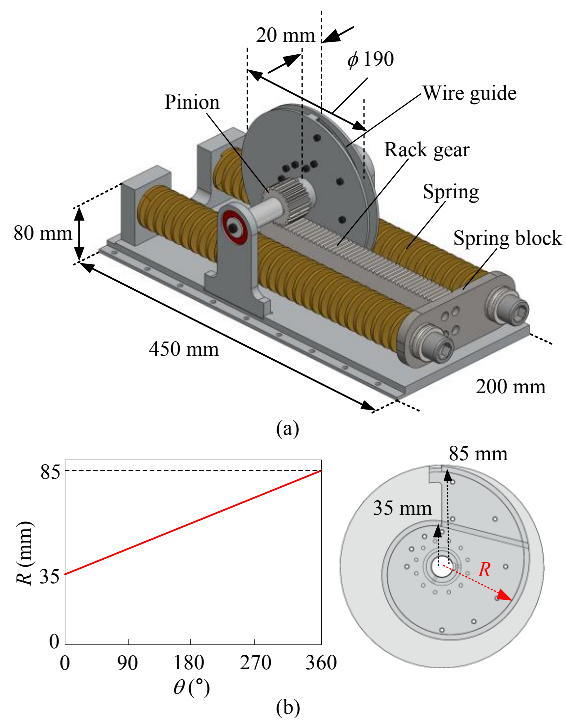


Figure 5. Design of proposed LGC: (a) total assembly, and (b) dimensions of the wire guide.

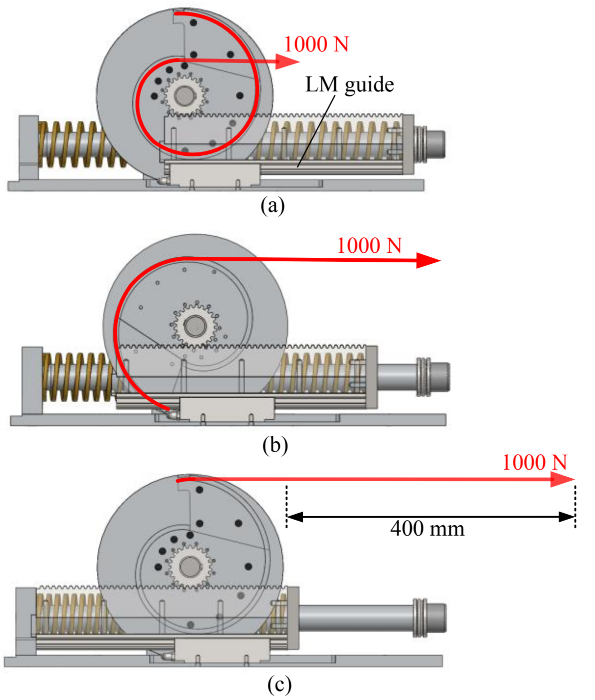


Figure 6. Operation of the wire guide: (a) initial state, (b) partially compressed state, and (c) fully compressed state.

## III. Verification

The LGC is fabricated as depicted in Fig. 7(a). The parts of the main body are made of aluminum alloy, and the rack-and-pinion is heat-treated and polished. The wire wound on the cam is a stainless steel wire of 3.18 mm in diameter that can withstand a tensile force of 9,000 N; it has a safety factor of nine for a maximum load of 1,000 N.

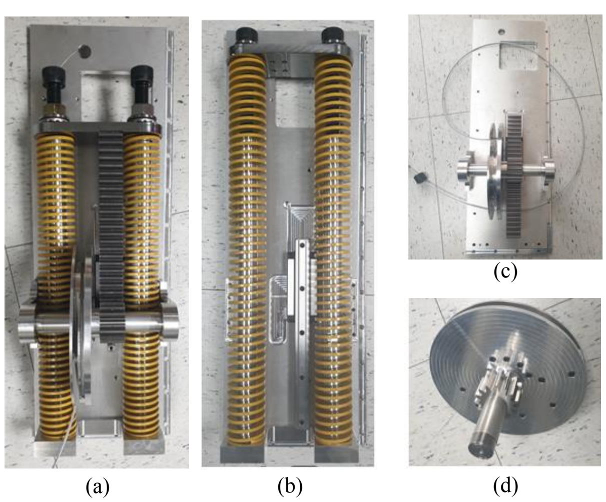


Figure 7. Manufactured LGC: (a) total assembly, (b) non-compressed spring and LM (linear motion) guide, (c) rack-pinion and wire, and (d) wire cam.

To verify the performance of the LGC, it is mounted on a lifting robot with prismatic joints, as depicted in Fig. 8. The wire extending through the cam of the LGC is wound around the pulley mounted on the top of the robot, and installed at the bottom of the robot's operating part. The lifting robot is a device that can lift a payload of 60 kg by driving a ball screw using a 200 W motor. In this study, an experiment is performed to lift a payload of 160 kg using the developed LGC. Additionally, to verify the uniformity of the LGC compensation force, the tensile force is measured by mounting a tensile load cell between the wire and the robot's operating part, as depicted in Fig. 9.

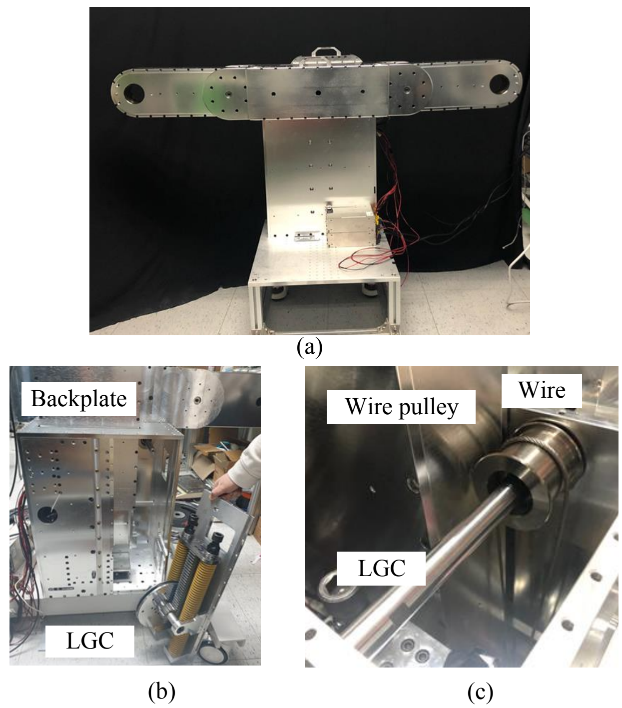


Figure 8. LGC installed on the lifting robot: (a) full view of the robot, (b) LGC installed on the backside, and (c) wire wound on the pulley.

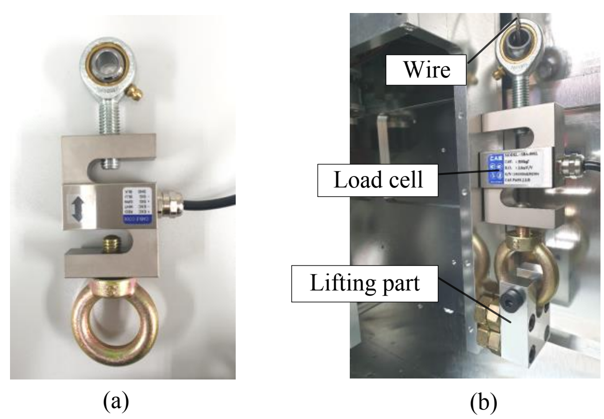


Figure 9. (a) Load cell and (b) experimental setup with load cell

Figure 10 depicts a graph of the three- phase motor current when a lifting robot lifts a 60 kg payload up and down by 400 mm without the assistance of the LGC. Figure 11 illustrates the graphs of three- phase current of the motor when lifting a 160 kg payload up and down, which is much larger than the original payload, by 400 mm with the LGC mounted on the robot. The comparison of Fig. 10(b) and Fig. 11(b) indicates that the motor currents in the two cases are almost identical, which implies that the loads applied to the motor are almost equal. This demonstrates that the compensation force generated by the LGC has the effect of a considerable payload increase of 100 kg.

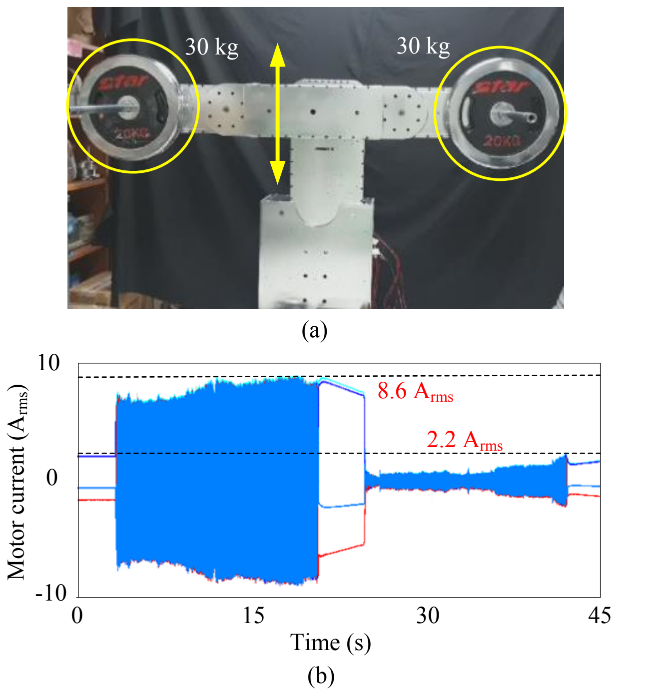


Figure 10. Lifting 60 kg payload up and down without LGC: (a) 60 kg load mounted on the robot, and (b) motor current during the task.

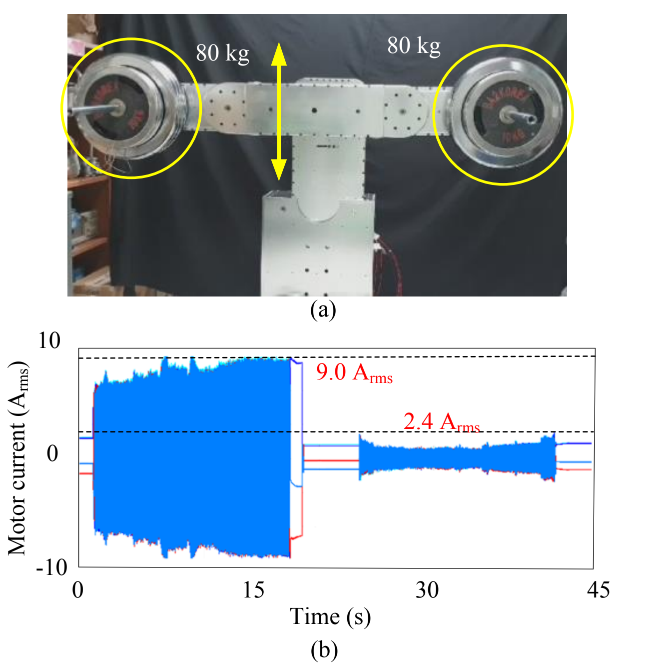


Figure 11. Lifting 160 kg payload up and down without LGC: (a) 160 kg load mounted on the robot, and (b) motor current during the task

The compensation force generated by the LGC can be obtained from the load cell data, as shown in Fig. 12. As shown in the graph, the LGC uniformly generates the target compensation force of 1,000 N with a maximum error of 4%. When lifting the payload up and down, some noise and an error of 30 to 40 N occurs in comparison with the stationary state, which is caused by frictional force generated from the LM guide and the wire guide of the gravity compensator. On the other hand, the compensation force is uniformly maintained at 960 N at rest. Therefore, the theoretical considerations in Sections 2 and 3 are valid.

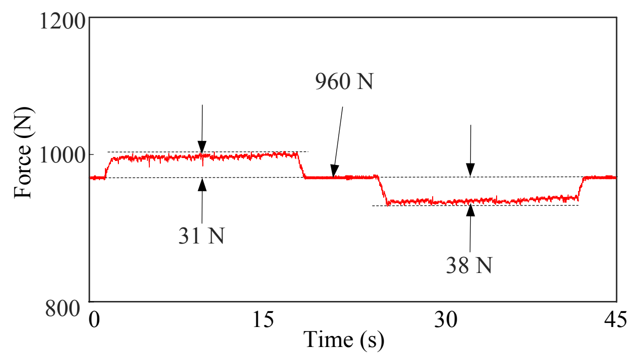


Figure 12. Compensation force of LGC measured by the load cell

## IV. Conclusion

In this study, we developed a high-capacity LGC comprising only mechanical elements, such as springs, a rack-and-pinion, a cam, and a wire. The proposed LGC was designed to generate a constant compensation force regardless of the payload position and guarantee a long service life by using durable coil springs. The actual LGC was fabricated and mounted on a lifting robot, and a series of experiments were conducted to investigate the performance of the gravity compensation and the uniformity of the compensation force. The following conclusions were drawn from the experimental results.

1) The compensation force generated by the LGC was uniformly maintained at 1,000 N throughout the travel range of the load, and the error was within 4%.

2) By installing the LGC in the lifting robot with a payload of 60 kg, the robot could lift a payload of 160 kg without a significant change in the motor torque, thus verifying the payload increase effect of 100 kg.

## References

[1] H. Diken, “Effect of mass balancing on the actuator torques of a manipulator,” Mechanism and Machine Theory, vol. 30, no. 4, pp. 495-500, 1995.

[2] J. M. Herve, “Device for counter-balancing the forces due to gravity in a robot arm,” U.S. Patent 4, 620, 829, 1986.

[3] K. Koser, "A cam mechanism for gravity-balancing," *Mechanics Research Communications*, vol. 36, no. 4, pp. 523-530, 2009.

[4] H. Ortmeier, D. Engelhardt, “Device and method for balancing the weight on a robot arm,” U.S. Patent No. 6, 408, 225, 2002.

[5] H. S. Kim, J. K. Min, and J. B. Song, “Multiple degree of freedom counterbalance robot arm based on slider-crank

mechanism and bevel gear units," *IEEE Transactions on Robotics*, vol. 32, no. 1, pp. 230-235, 2016.

[6] S. K. Agrawal and A. Fattah, "Gravity-balancing of spatial robotic manipulators," *Mechanism and machine theory*, vol. 39, no. 12, pp. 1331–1344, 2004.

[7] W. B. Lee, S. D. Lee, and J. B. Song, "Design of a 6-DOF collaborative robot arm with counterbalance mechanisms," *IEEE International Conference on Robotics and Automation*, pp. 3696-3791, 2017.

[8] D. Lee and T. Seo, "Lightweight multi-dof manipulator with wire-driven gravity compensation mechanism," IEEE/ASME Transactions on Mechatronics, vol. 22, no. 3, pp. 1308–1314, 2017.

[9] E. H. Berger and K. A. Wyrobek, "Humanoid robotics system and methods," U.S. Patent No. 13, 084, 380, 2012.

[10] Muscle Corporation, SASUKE, https://www.musclerobo.com.

[11] H. M. Guignard, "Spring-barrel supplying constant torque," U.S. Patent No. 5, 539, 708, 1996.

[12] T. G. Rogers, "Constant force compensation for power spring weight balance," U.S. Patent No. 5, 054, 162, 1991.

[13] E. F. Duval, "Mechanical arm including a counterbalance." U.S. Patent No. 7, 798, 035, 2010.